Mathematical analysis and numerical solution of models with dynamic Preisach hysteresis

A. Bermúdez[a], D. Gómez[a], P. Venegas[b]

[a]*Departamento de Matemática Aplicada, Universidade de Santiago de Compostela, E-15782 Santiago de Compostela, Spain*
[b]*GIMNAP, Departamento de Matemática, Universidad del Bío-Bío, Concepción, Chile*

Abstract

Hysteresis is a phenomenon that is observed in a great variety of physical systems, which leads to a nonlinear and multivalued behavior, making their modeling and control difficult. Even though the analysis and mathematical properties of several rate-independent and rate-dependent hysteresis models are known, this is not the case for the Bertotti's rate-dependent extension of the classical Preisach model; the so-called dynamic Preisach model for which current approaches lack a proper functional analytic framework which is essential to formulate optimization problems and develop stable numerics, both being crucial in practice. This paper deals with the description and mathematical analysis of the dynamic Preisach hysteresis model. Toward that end, we complete a widely accepted definition of the dynamic model commonly used to describe the constitutive relation between the magnetic field H and the magnetic induction B, in which, the values of B not only depends on the present values of H but also on the past history and its velocity. We first analyze mathematically some important properties of the model and compare them with known results for the static Preisach model. Then, we consider a parabolic problem with dynamic hysteresis motivated by electromagnetic field equations. Under suitable assumptions, we prove the existence of a solution of a weak formulation of the problem and solve it numerically. Finally, we report a numerical test in order to assess the order of convergence and to illustrate the behavior of the numerical solution for different configurations of the dynamic Preisach model.

Keywords: hysteresis, dynamic Preisach model, transient eddy current, finite element method

☆The work of the authors from Universidade de Santiago de Compostela was supported by Ministerio de Economía y Competitividad (Spain) under the research project ENE2013–47867–C2–1–R and by Ministerio de Economía, Industria y Competitividad (Spain) under the research project MTM2017-86459-R. P. Venegas was partially supported by FONDECYT project 11160186.

*Corresponding author

Email addresses: alfredo.bermudez@usc.es (A. Bermúdez), mdolores.gomez@usc.es (D. Gómez), pvenegas@ubiobio.cl (P. Venegas)

1. Introduction

Hysteresis is a nonlinear behavior exhibited by some media characterized by a special memory-based property according to which their response to particular changes is a function of the preceding responses. This characteristic is known as *memory effect*. A survey of hysteresis models can be found, for instance, in [32, 20, 47]. Detailed studies of these models have been done by different authors. From the mathematical point of view, we refer to the pioneering work of Krasnosel'skiǐ and Pokrovskiǐ [24], who introduced the fundamental concept of hysteresis operator and conducted a systematic analysis of the mathematical properties of these objects.

Models of hysteresis can be divided into two main classes: *static* or *rate-independent* and *dynamic* or *rate-dependent* models. In the former, the values of output depend just on the range of the input and on the order in which these values have been attained; in particular, the speed of the input has no influence [46]. As a consequence, the model cannot reflect the dependence with frequency or field waveform. This is a fundamental property of classical hysteresis phenomena and some authors consider that it is an essential feature of them (see [46]). Conversely, in dynamic hysteresis, the effect of the speed of changes of the applied input is added to the model. That is why dynamic models are also known as *rate-dependent* models.

The hysteresis phenomenon has been observed for a long time in many different areas of science and engineering. The term was initially coined in the area of magnetism [18] given that many ferromagnetic materials present hysteresis behavior that is reflected in the magnetization curves describing the magnetic response of the material to an applied magnetic field. From the electrical engineering point of view, having a good hysteresis model is fundamental to correctly estimate the energy losses in electrical machines, a very important issue to be taken into account when designing an electrical device. In particular, the so-called hysteresis and excess losses [3] would be provided by a hysteresis model. Consequently, numerical simulation of devices involving ferromagnetic materials is still quite a challenge.

One the of the most popular hysteresis operators among scientists and engineers is the classical Preisach model [40], a rate-independent model based on physical assumptions motivated by the concept of magnetic domains. Even if this model was first suggested in the area of ferromagnetism [35, 7, 39, 13], nowadays Preisach type operators [10] are recognized as a fundamental tool for describing a wide range of hysteresis phenomena in different subjects as elasto-plasticity [31], solid phase transitions [12], shape memory alloys [41], hydrology [23], fluid flow in porous media [43], infiltration [33], batteries [1], economics or biology [27], among others.

In the case of ferromagnetism, the original formulation of the classical Preisach model allows us to simulate scalar and rate-independent hysteresis relationship between the magnetic field H and the magnetic flux density B (or the magnetization M). Nevertheless, in many applications, the magnetization evolution was found to be dependent on the rate of applied field and thus, at present, there are several extensions of the classical Preisach model that behave like dynamic models. They are generically called *dynamic Preisach models* (see, for instance, [34, 6, 48, 14]).

On the other hand, the mathematical analysis of several rate-dependent and rate-independent hysteresis models has been addressed in classical reference books by Brokate and Sprekels [12], Krasnosel'skiĭ and Pokrovskiĭ [24], Visintin [46], and in other publications as Eleuteri [16, 17], Showalter [44], Bermúdez [4], Krejčí [26], Mielke [37], Gurevich [19] and Mayergoyz and Bertotti [7, 8, 35, 36]. However, to the best of the author's knowledge, this is not the case for the dynamic Preisach model proposed by Bertotti in [6], although there exist several publications devoted to the numerical solution of partial differential equations including this hysteresis model [15, 29, 2].

The goal of this work is twofold: the mathematical analysis of the dynamic Preisach model of hysteresis proposed in [6] and the mathematical analysis and numerical solution of parabolic problems with dynamic hysteresis, motivated by electromagnetic field equations. With this in mind, we first formalize the definition of the dynamic Preisach model, more specifically, we focus on the *dynamic relay* which is introduced as the solution of a multi-valued ordinary differential equation. As we will see later, this dynamic relay is also related to the so-called stop (or elastic-plastic) operator considered in [12, 24, 46] and previously by Moreau [38]. Then, we prove existence and uniqueness as well as some properties of the dynamic relay which allow us to obtain corresponding mathematical properties of the dynamic Preisach model. From these properties and by applying the same techniques as for problems modeled by the classical Preisach operator (see, for instance [46]), we prove existence of solution of a parabolic equation including the Bertotti's dynamic Preisach hysteresis model. Under further assumptions a uniqueness result is obtained.

The paper is organized as follows: in Section 2 we briefly recall the definition of the rate-independent relay operator and the classical Preisach operator; then, a new formulation of the dynamic (rate-dependent) relay operator is provided and some properties are proved. In Section 3, by using the dynamic relay, we recall the definition of the Bertotti's dynamic Preisach operator and prove some of its properties. An abstract parabolic problem with dynamic hysteresis is stated in Section 4. From the properties proved for the dynamic Preisach model, an existence result is derived. Finally, in Section 5 we introduce a numerical scheme to approximate the parabolic problem. We report two numerical tests: one in order to assess the order of convergence and another one to illustrate the behavior of the numerical solution for different configurations of the dynamic Preisach model. Finally, some conclusions are drawn.

2. Relays and Preisach operators

The Preisach model describes the hysteresis using a superposition of elementary hysteresis operators called *relay operators*. The model assumes that the material consists of an infinite number of (magnetic) particles each of them characterized by a relay. Thus, the whole system can be modeled by a weighted parallel connections of these relays. The weight function works as a local influence of each relay in the overall hysteresis operator. It needs to be estimated from measured data.

Depending on the characteristics of the relay and on the nature of the connection among them, different Preisach (or Preisach-type) models can be obtained. In what follows we briefly recall the definition of the rate-independent relay which is the basis of the classical Preisach model. Then, we introduce a rate-dependent or dynamic relay leading to the definition of the *dynamic Preisach* model introduced in [6].

2.1. The static (rate-independent) relay

In the classical (rate-independent) Preisach model, the output of each relay is represented by an elementary rectangular loop on the input-output diagram (u, v), with transition thresholds at ρ_1 and ρ_2 (see Figure 1 (left)).

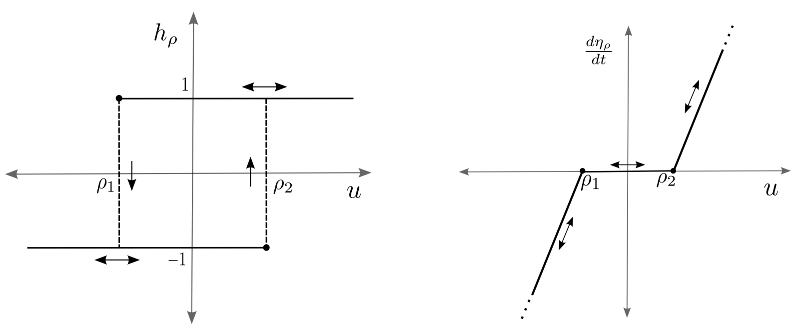

Figure 1: Relay in the (u, h_ρ)-plane for the classical Preisach model (left) and relay slope for the dynamic Preisach model for the case $|\eta_\rho| < 1$(right). The arrows indicate the authorized paths.

Formally, given any couple $\rho = (\rho_1, \rho_2)$ such that $\rho_1 < \rho_2$, the corresponding relay operator h_ρ is defined as follows: for any $u \in C([0, T])$ and $\xi \in \{1, -1\}$ (an initial condition), $h_\rho(u, \xi)$ is a function from $[0, T]$ to $\mathbb{R}$ such that, firstly,

$$h_\rho(u, \xi)(0) := \begin{cases} -1 & \text{if } u(0) \leq \rho_1, \\ \xi & \text{if } \rho_1 < u(0) < \rho_2, \\ 1 & \text{if } u(0) \geq \rho_2. \end{cases}$$

Secondly, for any $t \in (0,T]$, let us set $X_u(t) := \{\tau \in (0,t] : \ u(\tau) = \rho_1 \text{ or } \rho_2\}$. This set takes into account the previous instants in which u has got the thresholds ρ_1 or ρ_2. Let us define

$$h_\rho(u,\xi)(t) := \begin{cases} h_\rho(u,\xi)(0) & \text{if } X_u(t) = \emptyset\,, \\ -1 & \text{if } X_u(t) \neq \emptyset \quad \text{and} \quad u(\max X_u(t)) = \rho_1, \\ 1 & \text{if } X_u(t) \neq \emptyset \quad \text{and} \quad u(\max X_u(t)) = \rho_2. \end{cases} \tag{1}$$

We notice that h_ρ can only be equal to ± 1 depending on the past history of the system, with instantaneous "switch-down" and "switch-up" when u takes the values ρ_1 and ρ_2, respectively. The value of the relay operator remains at the last value (± 1) until u takes the value of one opposite switch, that is, switch to value 1 when u attains the value ρ_2 from below, and to -1 when it attains ρ_1 from above.

To define the *classical Preisach operator* $\mathcal{F}_S$, it is useful to introduce the so-called *Preisach triangle* $\mathcal{T} := \{\rho = (\rho_1,\rho_2) \in \mathbb{R}^2 : -\rho_0 \leq \rho_1 \leq \rho_2 \leq \rho_0\}$ where $\rho_0 > 0$ is given. Let us denote by Y the family of Borel measurable functions $\mathcal{T} \to \{-1,1\}$ and by ξ a generic element of Y. Then, $\mathcal{F}_S$ is given by

$$\begin{aligned} &\mathcal{F}_S : C([0,T]) \times Y \longrightarrow C([0,T]), \\ &(u,\xi) \longmapsto [\mathcal{F}_S(u,\xi)](t) = \int_{\mathcal{T}} [h_\rho(u,\xi(\rho))](t) p(\rho)\, d\rho, \end{aligned} \tag{2}$$

where $p \in \mathrm{L}^1(\mathcal{T})$, with $p > 0$, is termed *Preisach density function*. Thus, the classical Preisach model can be understood as the "sum" of a family of static relays, distributed with a certain density p. Considering the definition above, this operator is a hysteresis operator in the mathematical sense established by Visintin [46].

Remark 1. If $u = 0$ at $t = 0$, then we can consider the following initial condition:

$$h_\rho(u,\xi)(0) := \begin{cases} -1 & \text{if } \rho_1 + \rho_2 > 0 \\ 1 & \text{if } \rho_1 + \rho_2 < 0. \end{cases} \tag{3}$$

In electromagnetism, this initial configuration is usually called "demagnetized" or "virginal" state because it leads to a null magnetic induction when p is symmetric [35].

Currently, the classical Preisach model serves as a basis for generalizations that try to overcome some of the lacks of the model; in particular, the fact that the form of the hysteresis diagram does not reflect the frequency content of the input $u(t)$ (see (1) and (2)). In other words, the model is rate-independent [35] which means that, at any instant t, $[\mathcal{F}_S(u,\xi)](t)$ only depends on the image set $u([0,t])$ and on the order in which these values of u have been attained, but not on the rate of change of u. Formally, this can be expressed as follows [46].

Definition 1. A mapping $\zeta : \mathrm{Dom}(\zeta) \subset C([0,T]) \times [-1,1] \to C([0,T])$ is said *rate-independent* if the path of the pair $(u, \zeta(u,\xi))$ is invariant with respect to any increasing diffeomorphism $\varphi : [0,T] \to [0,T]$, i.e.,

$$\forall (u,\xi) \in \mathrm{Dom}(\zeta),$$
$$\zeta(u \circ \varphi, \xi) = \zeta(u,\xi) \circ \varphi \quad \text{in } [0,T].$$

In order to take into account the rate-dependent effects, in the following section we will introduce the so-called dynamic relay.

2.2. The dynamic relay

In the rate-dependent generalization of the Preisach model (the so-called *dynamic* Preisach model) introduced by Bertotti [6, 9], the relays are assumed to switch at a finite rate proportional to the difference between $u(t)$ and the switching values ρ_1 and ρ_2 (see Figure 1 (right)). In particular, this means that, contrary to the classical relay where only two states, -1 and 1, are possible, now all intermediate states in the interval $[-1,1]$ can be attained (see Figure 2 and Remark 2). The proportionality factor, denoted by k, is a material-dependent parameter.

Formally, for a fixed $\rho = (\rho_1, \rho_2) \in \mathbb{R}^2$, $\rho_1 < \rho_2$, and motivated by [6], we define the dynamic relay operator $\eta_\rho : \mathrm{L}^1(0,T) \times [-1,1] \to \mathrm{W}^{1,1}(0,T)$ such that, for any $u \in \mathrm{L}^1(0,T)$ and $\xi \in [-1,1]$, $\eta_\rho(u,\xi) : [0,T] \to [-1,1]$ is the unique function $y \in \mathrm{W}^{1,1}(0,T)$ such that $-1 \le y(t) \le 1$ and solves the nonlinear Cauchy problem:

$$\frac{dy}{dt}(t) = F(t, y(t)) := \begin{cases} k(u(t)-\rho_2)^+ - k(u(t)-\rho_1)^- & \text{if } -1 < y(t) < 1, \\ 0 & \text{if } y(t) = -1 \text{ and } u(t) \le \rho_2, \\ k(u(t)-\rho_2) & \text{if } y(t) = -1 \text{ and } u(t) \ge \rho_2, \\ k(u(t)-\rho_1) & \text{if } y(t) = 1 \text{ and } u(t) \le \rho_1, \\ 0 & \text{if } y(t) = 1 \text{ and } u(t) \ge \rho_1, \end{cases} \tag{4}$$

$$y(0) = \xi. \tag{5}$$

We have used the standard notations:

$$x^+ = \max\{x, 0\} \text{ and } x^- = \max\{-x, 0\},$$

so that $x = x^+ - x^-$. Notice that (4) partially coincides with the definition given in [6] when $-1 < y < 1$. Nevertheless, in order to perform a suitable mathematical analysis, we need to consider all the other cases included in (4). We also notice that this formulation and the one by Bertotti are consistent because cases third and fourth cannot happen, as we will see in the sequel.

Let $g_\rho : \mathbb{R} \to \mathbb{R}$ be defined by

$$g_\rho(u) := -k(u-\rho_1)^- + k(u-\rho_2)^+. \tag{6}$$

Then g is Lipschitz-continuous:

$$|g_\rho(u_1) - g_\rho(u_2)| \le k|u_1 - u_2|$$

and, therefore, if $u \in \mathrm{L}^1(0,T)$ then $g_\rho(u)$ also belongs to $\mathrm{L}^1(0,T)$. In terms of $g_\rho(u(t))$, (4) can be rewritten as follows

$$\frac{dy}{dt}(t) = \begin{cases} g_\rho(u(t)) & \text{if } -1 < y(t) < 1, \\ 0 & \text{if } y(t) = -1 \text{ and } g_\rho(u(t)) \le 0, \\ g_\rho(u(t)) & \text{if } y(t) = -1 \text{ and } g_\rho(u(t)) \ge 0, \\ g_\rho(u(t)) & \text{if } y(t) = 1 \text{ and } g_\rho(u(t)) \le 0, \\ 0 & \text{if } y(t) = 1 \text{ and } g_\rho(u(t)) \ge 0, \end{cases} \tag{7}$$

$$y(0) = \xi. \tag{8}$$

In order to prove the existence and uniqueness of such a function y, we will consider another *apparently different* initial-value problem, namely, find $y \in \mathrm{W}^{1,1}(0,T)$ satisfying $-1 \le y(t) \le 1$ and $q \in \mathrm{L}^1(0,T)$ such that

$$\begin{cases} \dfrac{dy}{dt}(t) = g_\rho(u(t)) - q(t), \\ y(0) = \xi, \end{cases} \tag{9}$$

and

$$\begin{cases} q(t) = 0 & \text{if } |y(t)| < 1, \\ q(t) \in (-\infty, 0] & \text{if } y(t) = -1, \\ q(t) \in [0, \infty) & \text{if } y(t) = 1. \end{cases} \tag{10}$$

Function $q(t)$ is a priori unknown and can be considered as a Lagrange multiplier associated with the constraint $|y(t)| \le 1$. In fact, problem (9)-(10) can be written in a more compact but equivalent way as a multi-valued ordinary differential equation:

$$\begin{cases} \dfrac{dy}{dt}(t) + \partial\chi_{[-1,1]}(y(t)) \ni g_\rho(u(t)), \\ y(0) = \xi, \end{cases} \tag{11}$$

where $\partial\chi_{[-1,1]}$ denotes the sub-differential of $\chi_{[-1,1]}$ which is the indicator function of interval $[-1,1]$. Let us recall that (see, for instance, [11])

$$\chi_{[-1,1]}(x) = \begin{cases} \infty & \text{if } |x| > 1, \\ 0 & \text{if } |x| \le 1, \end{cases} \qquad \text{and} \qquad \partial\chi_{[-1,1]}(x) = \begin{cases} [0,\infty) & \text{if } x = 1, \\ (-\infty, 0] & \text{if } x = -1, \\ 0 & \text{if } |x| < 1, \\ \emptyset & \text{if } |x| > 1. \end{cases}$$

Thus, it is easy to see that function $q(t)$ belongs to $\partial\chi_{[-1,1]}(y(t))$ for each $t \in [0,T]$ which means $|y(t)| \le 1$ and

$$q(t)\Big(z - y(t)\Big) \le 0 \quad \forall z \in \mathbb{R} \text{ with } |z| \le 1.$$

Indeed, we notice that the latter is equivalent to (10). Let us emphasize that function $q(t)$ is also an unknown of the problem and, as we will see below, it is unique too. Actually, the value of $q(t)$ accommodates so that the solution of the

Cauchy problem satisfies $|y(t)| \leq 1$, i.e., it is a Lagrange multiplier associated to this constraint. We also notice that the existence of a unique solution to the Cauchy problem (11) can be deduced from results proved in the much more general setting of differential equations in Hilbert spaces involving maximal monotone operators (see for instance [11]). However, for the sake of completeness we include a direct proof for this simpler case, based on the following trivial result:

Lemma 2.1. *Let $u \in \mathrm{L}^1(0,T)$ and $\xi \in [-1,1]$. Function $y \in \mathrm{W}^{1,1}(0,T)$ is a solution to problem* (11) *if and only if*

$$y(t) = \mathcal{S}[\int_0^{\{\}} g_\rho(u(t'))dt', \xi](t),$$

where g_ρ has been defined in (6) *and $\mathcal{S}$ denotes the so-called stop operator (also called elastic-plastic element) which is defined by*

$$\mathcal{S} : v \in \mathrm{W}^{1,1}(0,T) \to z \in \mathrm{W}^{1,1}(0,T),$$

where $z = \mathcal{S}v$ is the unique solution to the Cauchy problem

$$\begin{cases} \dfrac{dz}{dt}(t) + \partial\chi_{[-1,1]}(z(t)) \ni \dfrac{dv}{dt}(t), \\ z(0) = \xi. \end{cases} \tag{12}$$

Theorem 2.2. *Let us assume that u is a given function in $\mathrm{L}^1(0,T)$. Then for each $\xi \in [-1,1]$ there exists a unique function $y \in \mathrm{W}^{1,1}(0,T)$ satisfying (11). Consequently, function $q(t)$ defined almost everywhere by*

$$q(t) := -\frac{dy}{dt}(t) - k(u(t) - \rho_1)^- + k(u(t) - \rho_2)^+$$

belongs to $\mathrm{L}^1(0,T)$ and $q(t) \in \partial\chi_{[-1,1]}(y(t))$ a.e. in $(0,T)$.

Proof. *It is a consequence of the previous lemma, the fact that if $u \in \mathrm{L}^1(0,T)$ the function*

$$v(t) := \int_0^t g_\rho(u(t'))dt'$$

belongs to $\mathrm{W}^{1,1}(0,T)$, and well-known existence and uniqueness results for the stop operator that can be found in [38, Sect. 6.d] (see also [12, 24, 46]).

We also have the following characterization of $q(t)$.

Lemma 2.3. *For a.e. in $[0,T]$ we have,*

$$q(t) = P_{\partial\chi_{[-1,1]}(y(t))}\big(g_\rho(u(t))\big) = \begin{cases} 0 & \textit{if } -1 < y(t) < 1, \\ g_\rho(u(t)) & \textit{if } y(t) = -1 \textit{ and } g_\rho(u(t)) \leq 0, \\ 0 & \textit{if } y(t) = -1 \textit{ and } g_\rho(u(t)) \geq 0, \\ 0 & \textit{if } y(t) = 1 \textit{ and } g_\rho(u(t)) \leq 0, \\ g_\rho(u(t)) & \textit{if } y(t) = 1 \textit{ and } g_\rho(u(t)) \geq 0, \end{cases} \tag{13}$$

where $P_{\partial\chi_{[-1,1]}(y(t))}$ denotes the projection on the set $\partial\chi_{[-1,1]}(y(t))$.

Proof. It follows immediately from Remark 3.9 in [11]. $\square$

As a consequence of the previous characterization of $q(t)$ we obtain an equivalent expression for (9).

Corollary 2.4. *We have, a.e. in* $[0,T]$,

$$\frac{dy}{dt}(t) = g_\rho(u(t)) - q(t) = \begin{cases} g_\rho(u(t)) & \text{if } -1 < y(t) < 1, \\ 0 & \text{if } y(t) = -1 \text{ and } g_\rho(u(t)) \leq 0, \\ g_\rho(u(t)) & \text{if } y(t) = -1 \text{ and } g_\rho(u(t)) \geq 0, \\ g_\rho(u(t)) & \text{if } y(t) = 1 \text{ and } g_\rho(u(t)) \leq 0, \\ 0 & \text{if } y(t) = 1 \text{ and } g_\rho(u(t)) \geq 0, \end{cases} \tag{14}$$

and, therefore, the solution of (11) *is also a solution to the original problem* (4)-(5)*. This follows from* (14) *and the fact that* $g_\rho(u(t)) \leq 0$ *is equivalent to* $u(t) \leq \rho_2$ *and the same is true for* $g_\rho(u(t)) \geq 0$ *and* $u(t) \geq \rho_1$.

Let us introduce the Heaviside function H, namely, $\mathrm{H}(x) = 1$ if $x > 0$ and $\mathrm{H}(x) = 0$ if $x \leq 0$. The dynamic relay satisfies the following Hilpert's inequality [21].

Lemma 2.5. *Let* u_1 *and* u_2 *be two functions in* $\mathrm{L}^1(0,T)$ *and* $\xi \in [-1,1]$*. We define* $y_i = h_\rho(u_i, \xi)$, $i = 1,2$ *and introduce the differences* $u = u_2 - u_1$, $y = y_2 - y_1$*. Then* y^+ *belongs to* $\mathrm{W}^{1,1}(0,T)$ *and satisfies:*

$$\frac{d}{dt} y^+(t) \leq \frac{dy}{dt}(t)\mathrm{H}(u(t)) \qquad a.e\ t \in [0,T]. \tag{15}$$

Proof. From Theorem 2.2 it follows that $y \in \mathrm{W}^{1,1}(0,T)$ and therefore $y^+ \in \mathrm{W}^{1,1}(0,T)$. Moreover, it is known that $\frac{d}{dt}y^+(t) = \frac{dy}{dt}(t)\mathrm{H}(y(t))$ and thus, inequality (15) is equivalent to $\frac{dy}{dt}(t)\mathrm{H}(y(t)) \leq \frac{dy}{dt}(t)\mathrm{H}(u(t))$ a.e $t \in [0,T]$. Clearly this inequality holds when $\mathrm{H}(y(t)) = \mathrm{H}(u(t)) = 1$ and $\mathrm{H}(y(t)) = \mathrm{H}(u(t)) = 0$. To get the result it is enough to show that

a) if $\mathrm{H}(u(t)) = 1$ ($u_2(t) > u_1(t)$) and $\mathrm{H}(y(t)) = 0$ ($y_2(t) \leq y_1(t)$), then $\frac{dy}{dt}(t) \geq 0$ and,

b) if $\mathrm{H}(u(t)) = 0$ ($u_2(t) \leq u_1(t)$) and $\mathrm{H}(y(t)) = 1$ ($y_2(t) > y_1(t)$), then $\frac{dy}{dt}(t) \leq 0$.

To determine the sign of $\frac{dy}{dt}(t)$ in *a*), we consider the definition of $\frac{dy_i}{dt}$ (cf. (14)), $i = 1,2$

$$\frac{dy_i}{dt}(t) = \begin{cases} g_\rho(u_i(t)) & \text{if } -1 < y_i(t) < 1, \\ 0 & \text{if } y_i(t) = -1 \text{ and } u_i(t) \leq \rho_2, \\ 0 & \text{if } y_i(t) = 1 \text{ and } u_i(t) \geq \rho_1, \end{cases} \tag{16}$$

and notice that, since g_ρ is nondecreasing, $\frac{dy}{dt}(t) \geq 0$ when $|y_i| < 1$. Now we study the remaining cases:

- If $-1 < y_1(t) < 1$, then $y_2(t) \leq y_1(t) < 1$. If $y_2(t) = -1$ and $u_2(t) \leq \rho_2$, since $u_1(t) < u_2(t)$ we obtain that $g_\rho(u_1(t)) \leq 0 = \partial_t y_2(t)$. From the above and (16) it follows that $\partial_t y_1(t) \leq \partial_t y_2(t)$.
- If $y_1(t) = -1$ and $u_1(t) \leq \rho_2$, then $-1 \leq y_2(t) \leq y_1(t) = -1$ and thus $\partial_t y_1(t) = \partial_t y_2(t) = 0$.
- If $y_1(t) = 1$ and $u_1(t) \geq \rho_1$, then $u_2(t) > u_1(t) \geq \rho_1$ and $y_2(t) \leq y_1(t) = 1$. Notice that $g_\rho(u_2(t)) \geq 0$ since $u_2(t) > \rho_1$. Therefore $\partial_t y_1(t) = 0 \leq \partial_t y_2(t)$.

From the previous analysis we get that *a*) holds true. The case *b*) follows from *a*) by interchanging the roles of u_1 and u_2. □

From the previous analysis it follows that, for a given input u and initial state ξ, the dynamic relay can be computed by solving the multi-valued ordinary differential equation (11). This can be done, for instance, by using semi-smooth Newton [22] or Bermúdez-Moreno method [5], just to name a few. However, motivated by [6], we notice that for an input $u \in C([0,T])$ such that $X_u(T) = \{t_u^1, \ldots, t_u^M\}, M \geq 1$, if we define $t_u^0 := 0$ and $t_u^{M+1} := T$, then the dynamic relay $y := \eta_\rho(u, \xi)$ can be obtained by integrating (14) (equivalently (4)) with respect to t and taking into account the constraint $-1 \leq y \leq 1$. Notice that, for each $t \in (t_u^m, t_u^{m+1}], m = 0, \ldots, M+1$, $y(t)$ is either nondecreasing (if $u(t) \geq \rho_2$), or nonincreasing (if $u(t) \leq \rho_1$) or constant (if $\rho_1 \leq u(t) \leq \rho_2$). For ease of presentation, in order to obtain an expression for $y(t)$, we consider the first interval, namely, $t \in (t_u^0, t_u^1]$. In this case it follows that,

- If $\rho_1 \leq u(t) \leq \rho_2$ then, from (14), the slope of y vanishes along the interval. Thus, $y(t) = y(t_u^0) = \xi$ on $(t_u^0, t_u^1]$.
- If $u(t) \geq \rho_2$ then $y(t)$ increases but cannot exceed 1. Notice that the third case in (14) cannot be fulfilled on $(t_u^0, t_u^1]$, because when $y(t_u^0) = -1$ the slope of y is positive and $y(t) > -1, t \in (t_u^0, t_u^1]$. Thus, if $|y| < 1$ or $y = 1$, from the first and fifth cases in (14), respectively, we arrive at

$$y(t) = \min \left\{ 1, y(t_u^0) + \int_{t_u^0}^{t} k(u(s) - \rho_2) ds \right\}.$$

- If $u(t) \leq \rho_1$, then $y(t)$ decreases but cannot be less than -1. Similar to the previous case, we notice that the fourth case in (14) cannot be fulfilled on $(t_u^0, t_u^1]$ because when $y(t_u^0) = 1$ the slope of y is negative and $y(t) < 1, t \in (t_u^0, t_u^1]$. Thus, if $|y| < 1$ or $y = -1$, from the first and second cases in (14), respectively, we arrive at

$$y(t) = \max \left\{ -1, y(t_u^0) + \int_{t_u^0}^{t} k(u(s) - \rho_1) ds \right\}.$$

Thus, by proceeding similarly with the remaining intervals, it follows that for $t \in (t_u^m, t_u^{m+1}], m = 0, \dots, M$:

$$y(t) = \begin{cases} \min\left\{1, y(t_u^m) + \displaystyle\int_{t_u^m}^{t} k(u(s) - \rho_2)ds\right\} & \text{if } u(s) \geq \rho_2 \text{ for } s \in (t_u^m, t], \\ \max\left\{-1, y(t_u^m) + \displaystyle\int_{t_u^m}^{t} k(u(s) - \rho_1)ds\right\} & \text{if } u(s) \leq \rho_1 \text{ for } s \in (t_u^m, t], \\ y(t_u^m) & \text{otherwise.} \end{cases} \tag{17}$$

To give an idea of the plane curve $t \in [0, T] \to (u(t), y(t))$, we consider two examples with a sinusoidal input $u(t) = 200\sin(2\pi f t)$ and initial condition $\xi = -1$. This input is depicted in Figure 2 (top and bottom left) for frequency $f =$ 20Hz, where the dotted lines represent different (ρ_1, ρ_2) values. Figure 2 (top right) shows the curve $t \in [0, T] \to (u(t), y(t))$ when the relay η_ρ is characterized by switching values $(\rho_1, \rho_2) = (50, 100)$ and slopes $k \in \{1, 50, 10^8\}$. For the same slopes, in Figure 2 (bottom right) we show this curve for switching values $(\rho_1, \rho_2) = (-50, 50)$. Notice that $(u(t), y(t))$ may vary in an asymmetric way when the input is not symmetric with respect to (ρ_1, ρ_2) (see dashed line in Figure 2 (top right)). We also notice that the dash-dotted line in Figure 2 (top and bottom right) becomes similar to the discontinuous relay of the classical Preisach model (see Figure 1 (left)), that is, the classical relay can be seen as the limit as $k \to \infty$ of the dynamic relay.

For the second example we analyze the evolution of the relays with a sinusoidal input $u(t) = 200\sin(2\pi f t)$ for $k = 50$ and different frequencies f. Figure 3 shows the dynamic relays characterized by $(\rho_1, \rho_2) = (50, 100)$ (top right) and $(\rho_1, \rho_2) = (-50, 50)$ (bottom right) for frequencies 50, 500 and 5000 Hz. From these examples we can see the variation of the dynamic relay with respect to k and the input rate. In particular, Figure 3 shows that the dynamic relay is rate-dependent.

Remark 2. Unlike the classical Preisach model, in the dynamic model the initial state ξ belongs to $[-1, 1]$ instead of $\{-1, 1\}$. Figure 4 shows the relays for $u_1(t) = 150\sin(2\pi f t)$ and $u_2(t) = 150\sin(2\pi f t) + 75$, with $f = 20$ Hz and two different initial states: $\xi_1 = -0.5$ (left) and $\xi_2 = 0.5$ (right). Two slopes are considered for each initial state: $k = 5$ and $k = 50$.

From the previous examples we notice that, unlike the classical static relay, the dynamic relay η_ρ does not satisfy either the so-called *rate independence* (see Definition 1) or the *piecewise monotonicity* properties defined as follows:

Definition 2. ζ is said *piecewise monotone* if when u is either nondecreasing or nonincreasing in $[t_1, t_2] \subset [0, T]$ then so is $\zeta(u, \xi)(t)$.

Notice that the dashed curve on Figure 3 (right) shows that the latter is not satisfied by the dynamic relay.

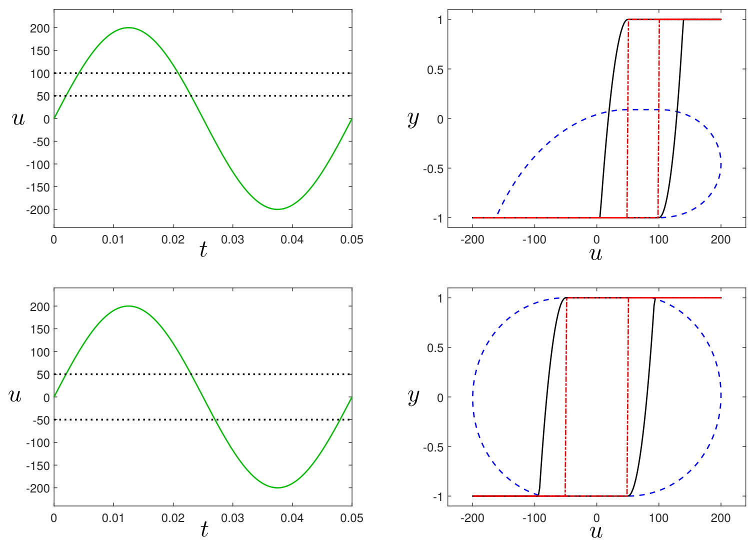

Figure 2: Input function $u(t) = 200\sin(2\pi f t)$ (left) for frequency $f = 20$Hz. Two dynamic relays are presented for switching values $(\rho_1, \rho_2) = (50, 100)$ (top), $(\rho_1, \rho_2) = (-50, 50)$ (bottom) and initial state $\xi = -1$. The switching values are represented by dotted lines on the left panels. The right panels show different relays with slopes $k = 1$ (dashed line), $k = 50$ (solid line) and $k = 10^8$ (dash-dotted line).

In the sequel we will show some properties of the dynamic relay solution to (4)-(5). The following lemma shows that, similar to the classical relay, the dynamic relays "preserves the order" of the inputs.

Lemma 2.6. *Let $u_1, u_2 \in \mathrm{L}^1(0,T)$, $\xi_1, \xi_2 \in [-1,1]$ and $k > 0$. The dynamic relay η_ρ satisfies the following order preservation property:*

$$\text{If } u_1 \leq u_2 \text{ a.e. in } [0,T] \text{ and } \xi_1 \leq \xi_2, \text{ then } [\eta_\rho(u_1,\xi_1)](t) \leq [\eta_\rho(u_2,\xi_2)](t) \ \forall t \in [0,T]. \tag{18}$$

Proof. Let $y_i(t)$ be the solution to problem (11) for $u = u_i(t)$, $i = 1,2$ and respective initial condition $y_i(0) = \xi_i$, $i = 1,2$. Then we have

$$\frac{dy_1}{dt} - \frac{dy_2}{dt} + q_1(t) - q_2(t) = g_\rho(u_1(t)) - g_\rho(u_2(t)), \tag{19}$$

$y_1(0) - y_2(0) = \xi_1 - \xi_2$ and $q_i(t) \in \partial\chi_{[-1,1]}(y_i(t))$, $i = 1,2$. Let us multiply (19) by $\big(y_1(t) - y_2(t)\big)^+ \in \mathrm{L}^\infty(0,T)$. We get

$$\frac{1}{2}\frac{d}{dt}|\big(y_1(t) - y_2(t)\big)^+|^2 + (q_1(t) - q_2(t))\big(y_1(t) - y_2(t)\big)^+$$
$$= \big(g_\rho(u_1(t)) - g_\rho(u_2(t))\big)\big(y_1(t) - y_2(t)\big)^+ \leq 0.$$

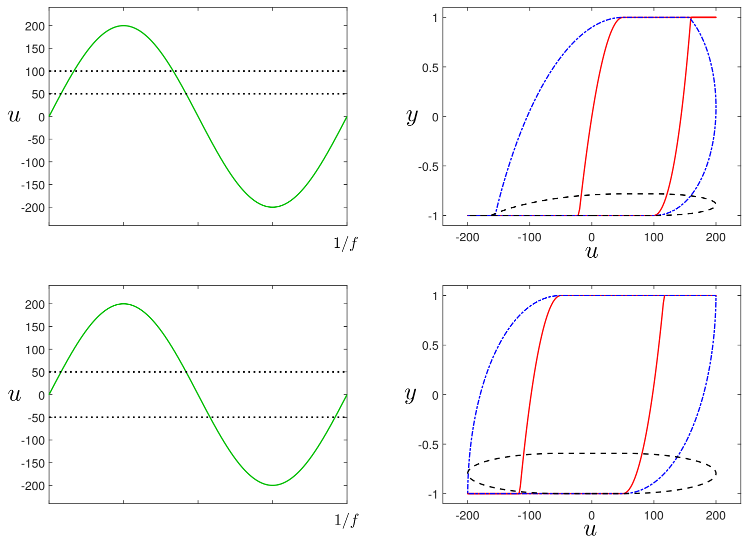

Figure 3: Input function $u(t) = 200\sin(2\pi f t)$ (left) for a fixed frequency denoted by f. Two dynamic relays are presented for switching values $(\rho_1, \rho_2) = (50, 100)$ (top), $(\rho_1, \rho_2) = (-50, 50)$ (bottom) and initial state $\xi = -1$. The switching values are represented by dotted lines on the left panels. The figures at the right show the (u, y) curve corresponding to the dynamic relay for $k = 50$ and three frequencies: $f = 50$Hz (dashed line), $f = 500$Hz (dash-dotted line) and $f = 5000$Hz (solid line).

By integrating from 0 to T and using the monotonicity of $\partial\chi_{[-1,1]}$ we deduce

$$\frac{1}{2}|\big(y_1(t) - y_2(t)\big)^+|^2 \leq \frac{1}{2}|\big(y_1(0) - y_2(0)\big)^+|^2 = \frac{1}{2}|\big(\xi_1 - \xi_2\big)^+|^2 = 0$$

Hence $\big(y_1(t) - y_2(t)\big)^+ = 0$ from which the result follows. $\square$

As a consequence of the previous result, the following property, to be used in the sequel, holds true.

Corollary 2.7. *Let $\xi \in [-1, 1]$ and $u, v \in \mathrm{L}^1(0, T)$ such that $u(t) = v(t)$ a.e. in $[0, t_1]$. If $u \geq v$ a.e. in $[t_1, t_2]$, $t_1 \leq t_2$, then*

$$([\eta_\rho(u, \xi)](t) - [\eta_\rho(v, \xi)](t))\,(u(t) - v(t)) \geq 0 \;\; a.e. \;\; in \;[t_1, t_2]. \tag{20}$$

The following lemma establishes a continuity property of dynamic relays.

Lemma 2.8. *Let $k > 0$ be given. Then the operator*

$$\eta_\rho : \mathrm{L}^1(0, T) \times [-1, 1] \to \mathrm{W}^{1,1}(0, T)$$

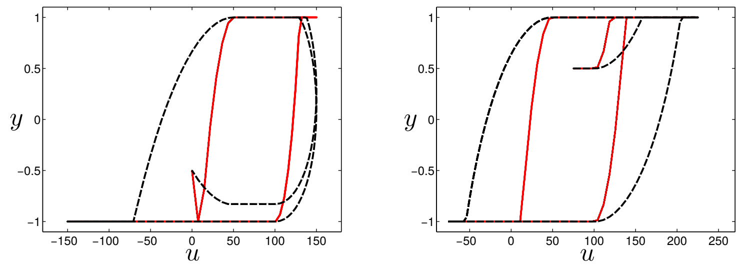

Figure 4: The left panel shows a dynamic relay corresponding to the input $u_1(t) = 150\sin(2\pi ft)$ and initial state $\xi = -0.5$. The right panel shows a dynamic relay corresponding to input $u_2(t) = 150\sin(2\pi ft) + 75$ and initial state $\xi = 0.5$. For both relays $f = 20$ Hz; two slopes, $k = 50$ (solid line) and $k = 5$ (dashed line) are considered.

is Lipschitz-continuous. More precisely, let u_1, u_2 *be any functions in* $\mathrm{L}^1(0,T)$, $\xi_1, \xi_2 \in [-1,1]$, *and* y_1, $y_2 \in \mathrm{W}^{1,1}(0,T)$ *their respective solutions of the Cauchy problem (11). Then we have*

$$\|y_1 - y_2\|_{\mathrm{W}^{1,1}(0,T)} \leq C(T)\Big(|\xi_1 - \xi_2| + k\|u_1 - u_2\|_{\mathrm{L}^1(0,T)}\Big). \tag{21}$$

Proof. Firstly, we notice that function $v(t) := \int_0^t g_\rho(u(s))\,ds$ belongs to the space $W^{1,1}(0,T)$. Then, the results follows from the global Lipschitz-continuity of the stop operator that has been proved in [28] (see also [12, Lemma 2.3.6] or [25, Prop. 1.1., Ch.II]).

□

3. Dynamic Preisach model

In this section we introduce the dynamic Preisach operator and prove some properties which are similar to the ones satisfied by the classical Preisach operator. Given $\rho_0 > 0$, let us consider again the *Preisach triangle* $\mathcal{T} := \{\rho = (\rho_1, \rho_2) \in \mathbb{R}^2 : -\rho_0 \leq \rho_1 \leq \rho_2 \leq \rho_0\}$ (see Figure 5 (left)) and the *Preisach function* $p \in \mathrm{L}^1(\mathcal{T})$ with $p > 0$. We denote by Y the convex set of initial configurations which can be defined by

$$Y := \big\{v \in L^1_p(\mathcal{T}) : |v(\rho)| \leq 1, \text{ a.e. } \rho \in \mathcal{T}\big\}$$

where

$$L^1_p(\mathcal{T}) := \{\xi : \mathcal{T} \to \mathbb{R} \text{ Lebesgue-measurable such that } \int_{\mathcal{T}} |\xi(\rho)|p(\rho)\,d\rho < \infty\}$$

endowed with the norm

$$\|\xi\|_{L^1_p(\mathcal{T})} := \int_{\mathcal{T}} |\xi(\rho)| p(\rho)\, d\rho.$$

Let us define the dynamic Preisach operator (see [6])

$$\begin{aligned} &\mathcal{F}_D : \mathrm{L}^1(0,T) \times Y \longrightarrow \mathrm{W}^{1,1}(0,T), \\ &(u,\xi) \longmapsto [\mathcal{F}_D(u,\xi)](t) = \int_{\mathcal{T}} [\eta_\rho(u,\xi(\rho))](t) p(\rho)\, d\rho. \end{aligned} \tag{22}$$

Notice that, if η_ρ is replaced by h_ρ given by (1) then we obtain the classical, rate-independent, Preisach model.

Mathematical properties of the classical Preisach operator are well known (see, for instance, [46]) but this is not the case for the dynamic model (22). From lemmas 2.5, 2.6 and 2.8 we obtain the following properties of the dynamic Preisach model.

Lemma 3.1. *The dynamic Preisach operator* $\mathcal{F}_D : \mathrm{L}^1(0,T) \times Y \longrightarrow \mathrm{W}^{1,1}(0,T)$ *is order preserving* (*cf.* (18)) *and satisfies the following properties:*

- *It is Lipschitz-continuous; more precisely, for all* $u_1, u_2 \in \mathrm{L}^1(0,T)$ *and* $\xi_1, \xi_2 \in Y$,

$$\begin{aligned} &\|\mathcal{F}_D(u_1,\xi_1) - \mathcal{F}_D(u_2,\xi_2)\|_{\mathrm{W}^{1,1}(0,T)} \\ &\qquad \leq C(T) \left(\|\xi_1 - \xi_2\|_{\mathrm{L}^1_p(\mathcal{T})} + k \|u_1 - u_2\|_{\mathrm{L}^1(0,T)} \int_{\mathcal{T}} p(\rho)\, d\rho \right). \end{aligned}$$

- *It is bounded in the following sense: for all* $v \in \mathrm{L}^1(0,T)$ *and* $\xi \in Y$,

$$\|\mathcal{F}_D(v,\xi)\|_{\mathrm{L}^\infty(0,T)} \leq \int_{\mathcal{T}} p(\rho)\, d\rho. \tag{23}$$

- *Given* $u_1, u_2 \in \mathrm{L}^1(0,T)$ *and* $\xi \in Y$, *we define* $w_i = \mathcal{F}_D(u_i,\xi)$, $i = 1,2$. *Let us introduce the differences* $u = u_2 - u_1$ *and* $w = w_2 - w_1$, *then*

$$\frac{d}{dt} w^+(t) \leq \frac{dw}{dt}(t) \mathrm{H}(u(t)) \qquad a.e\ t \in [0,T]. \tag{24}$$

Proof. The order preserving property is a consequence of Lemma 2.6 and the positivity of the Preisach function p.

The Lipschitz-continuity follows from Lemma 2.8. Indeed, we have

$$\begin{aligned} \|\mathcal{F}_D(u_1,\xi_1) - \mathcal{F}_D(u_2,\xi_2)\|_{\mathrm{W}^{1,1}(0,T)} &\leq \int_{\mathcal{T}} \|\eta_\rho(u_1,\xi_1(\rho)) - \eta_\rho(u_2,\xi_2(\rho))\|_{\mathrm{W}^{1,1}(0,T)} p(\rho)\, d\rho \\ &\leq C(T) \left(\int_{\mathcal{T}} |\xi_1(\rho) - \xi_2(\rho)| p(\rho)\, d\rho + k \|u_1 - u_2\|_{\mathrm{L}^1(0,T)} \int_{\mathcal{T}} p(\rho)\, d\rho \right), \end{aligned}$$

from which the result follows.

Finally (23) and (24) are consequences of the fact that $|\eta_\rho(u,\xi(\rho))(t)| \leq 1\ \forall t \in [0,T]$ and Lemma 2.5, respectively. □

As mentioned, in the classical Preisach model the relay h_ρ only takes values $+1$ or -1. Thus, at each time $t \geq t^0$, the Preisach triangle $\mathcal{T}$ is subdivided into two sets (one possibly empty):

$$S_u^-(t) := \{(\rho_1, \rho_2) \in \mathcal{T} : [h_\rho(u,\xi)](t) = -1\}\,,\; S_u^+(t) := \{(\rho_1, \rho_2) \in \mathcal{T} : [h_\rho(u,\xi)](t) = 1\}\,,$$

and consequently

$$[\mathcal{F}_S(u,\xi)](t) = \int_{S_u^+(t)} p(\rho)\, d\rho - \int_{S_u^-(t)} p(\rho)\, d\rho.$$

However, this is not the case for the dynamic model where the relays vary at finite rate between -1 and 1. Figure 6 shows the classical and dynamic relay configuration with respect to the same input u depicted in Figure 6 (top left). For this example we have considered a Preisach triangle characterized by $\rho_0 = 300$, a constant $k = 50$ and the demagnetized state as initial condition (cf. (1)).

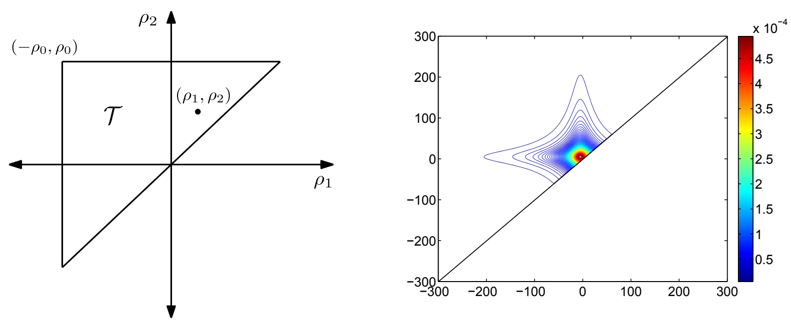

Figure 5: Preisach triangle (left) and Factorized-Lorentzian distribution p (right) with $N = 1/2000$, $\omega = 5$ and $\gamma = 4$.

We also compute the dynamic Preisach operator $\mathcal{F}_D(u,\xi)$ for u depicted in Figure 6 (top left) for different k values and frequencies. For the dynamic relay we have considered $k = 50$ and the Preisach function p is given by the Factorized-Lorentzian distribution [7] (see Figure 5 (right)):

$$p(\rho_1, \rho_2) := N\left(1 + \left(\frac{\rho_2 - \omega}{\gamma\omega}\right)^2\right)^{-1}\left(1 + \left(\frac{\rho_1 + \omega}{\gamma\omega}\right)^2\right)^{-1} \tag{25}$$

with $N = 1/2000$, $\omega = 5$ and $\gamma = 4$. Figure 7 shows the dynamic curve $(u, \mathcal{F}_D(u,\xi))$ for different k values and input velocities.

Finally, since we are interested in the mathematical analysis and computation of distributed electromagnetic models (also called field models) so following [46] we introduce a space-time dependent operator. Let Ω be a bounded domain

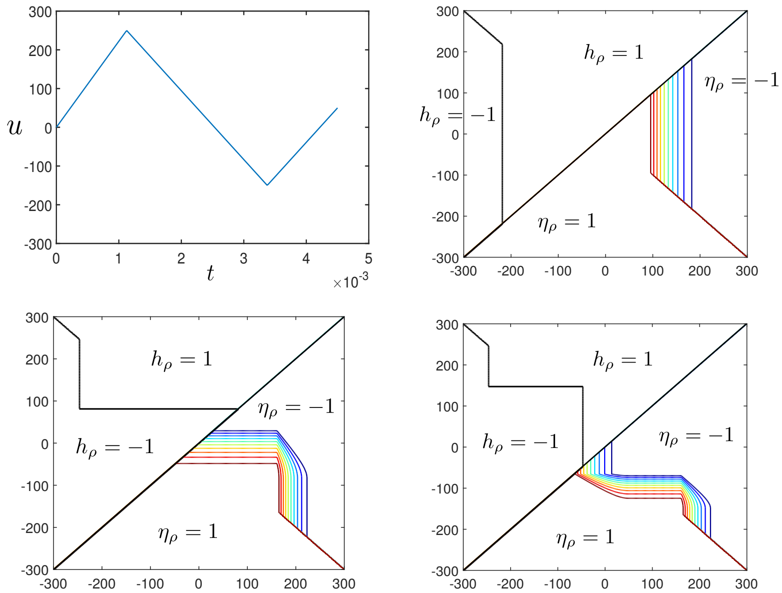

Figure 6: Input function $u(t)$ (top left) defined in $[0, 0.0045]$. The isolines correspond to the dynamic relay values η_ρ for $k = 50$ and to the classical relay h_ρ, at $t = 0.001$ (top right), $t = 0.003$ (bottom left) and t= 0.0045 (bottom right). For compactness we have considered the dynamic and classical relay in the same figure.

in $\mathbb{R}^d$. For $x \in \Omega$ let us give a time dependent function $u(x, \cdot) \in \mathrm{L}^1(0, T)$ and an initial state $\xi(x) \in Y$. We define a space and time dependent hysteresis operator $\mathcal{F} : \mathrm{L}^1(0, T; \mathrm{L}^2(\Omega)) \times \mathrm{L}^2(\Omega; Y) \to \mathrm{L}^\infty(0, T; \mathrm{L}^2(\Omega))$ as follows:

$$[\mathcal{F}(u, \xi)](x, t) := [\mathcal{F}_D(u(x, \cdot), \xi(x))](t) \quad \text{a.e. in } [0, T] \times \Omega, \tag{26}$$

where $\mathrm{L}^2(\Omega; Y)$ is a subset of $\mathrm{L}^2(\Omega; \mathrm{L}^1_p(\mathcal{T}))$, the space of all measurable functions $v : \Omega \to \mathrm{L}^1_p(\mathcal{T})$ such that

$$\|v\|_{\mathrm{L}^2(\Omega; \mathrm{L}^1_p(\mathcal{T}))} := \left(\int_\Omega \|u\|^2_{\mathrm{L}^1_p(\mathcal{T})} \right)^{1/2} < \infty.$$

Let us emphasize that operator $\mathcal{F}$ is local in x but non-local in t. We end this section with the following properties of dynamic operator $\mathcal{F}$ which follow from Lemma 3.1.

Lemma 3.2. *The dynamic Preisach operator* $\mathcal{F} : \mathrm{L}^1(0, T; \mathrm{L}^2(\Omega)) \times \mathrm{L}^2(\Omega; Y) \to \mathrm{L}^\infty(0, T; \mathrm{L}^2(\Omega))$ *is uniformly bounded, order preserving (cf. (18)) and Lipschitz-continuous in the following sense: there exists C depending on k such that, for*

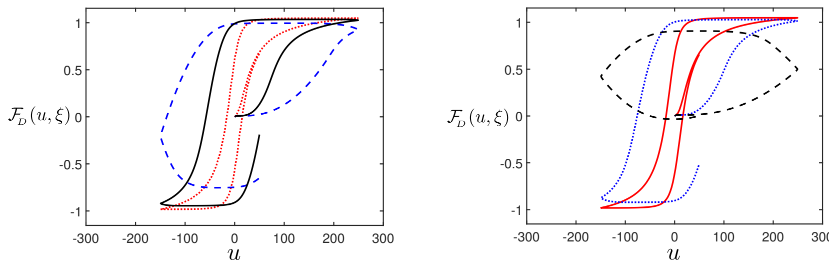

Figure 7: Dynamic Preisach hysteresis curve $\mathcal{F}_D$ for a Factorized-Lorentzian distribution, different k values and input $u(t)$ depicted on Figure 6 (top left). Left: input u defined in $[0, 0.0045]$ and slope values $k = 25$ (dashed line), $k = 200$ (solid line) and $k = 10^8$ (dotted line). Right: slope value $k = 100$ and input function $u(t)$ defined in $[0, 4.5]$ (solid line), $[0, 0.0045]$ (dotted line) and $[0, 0.00045]$ (dashed line).

all $u_1, u_2 \in \mathrm{L}^1(0,T;\mathrm{L}^2(\Omega))$ *and* $\xi_1, \xi_2 \in \mathrm{L}^2(\Omega; Y)$

$$\|\mathcal{F}(u_1,\xi_1) - \mathcal{F}(u_2,\xi_2)\|_{\mathrm{L}^\infty(0,T;\mathrm{L}^2(\Omega))} \leq C\left(\|\xi_1 - \xi_2\|_{\mathrm{L}^2(\Omega;\mathrm{L}^1_p(\mathcal{T}))} + \|u_1 - u_2\|_{\mathrm{L}^1(0,T;\mathrm{L}^2(\Omega))}\right).$$

4. Parabolic problem with dynamic hysteresis

In this section we introduce a parabolic problem with dynamic hysteresis for which we state an existence result by using the properties proved in the previous section. A particular case of this abstract problem arising from numerical simulation of eddy currents in ferromagnetic hysteretic materials is considered in Example 4.2 below.

Let $T > 0$ and $\Omega \in \mathbb{R}^d, d = 2, 3$ be a bounded domain with smooth boundary $\Gamma = \partial\Omega$. Let $V \subset H$ be two Hilbert spaces of scalar functions defined in Ω with continuous, dense, compact embedding. Then we have $V \subset H \equiv H' \subset V'$. We consider a mapping $a : (0,T) \times V \times V \to \mathbb{R}$ such that $a(t,\cdot,\cdot)$ is bilinear a.e. $t \in (0,T)$. We are interested in the mathematical analysis of the following parabolic problem: find $u \in \mathrm{L}^2(0,T;V) \cap \mathrm{L}^\infty(0,T;H)$ with $\partial_t u \in \mathrm{L}^2(0,T;V')$, and $w \in \mathrm{L}^2(0,T;H)$ with $\partial_t w \in \mathrm{L}^2(0,T;V')$, such that

$$\langle \partial_t u + \partial_t w, v\rangle_{V,V'} + a(t,u,v) = \langle f, v\rangle_{V,V'} \quad \forall v \in V, \quad \text{a.e. in } (0,T], \tag{27a}$$

$$w = \mathcal{F}(u,\xi) \qquad \text{in } \Omega \times [0,T], \tag{27b}$$

$$(u+w)(0) = u_0 + w_0 \qquad \text{in } \Omega. \tag{27c}$$

Here, operator $\mathcal{F}$ is defined by (26). We introduce the following assumptions that will be used to prove the existence of a solution to (27):

H.1 $a(\cdot,u,v)$ is a continuous form in $V\times V$. Moreover, it is Lipschitz continuous in t and satisfies the Gårding's inequality

$$a(t,v,v)+\lambda\|G\|_H^2 \geq \gamma\|G\|_V^2 \quad \forall v\in V, \quad \forall t\in[0,T], \tag{28}$$

for some constants $\lambda,\gamma\geq 0$.

H.2 f belongs to $\mathrm{H}^1(0,T;V')$, $u_0\in V$ and $w_0:=\mathcal{F}(u_0)\in H$.

H.3 For a fixed initial state $\xi:\Omega\to Y$, the mapping $\mathcal{F}:\mathrm{L}^2(0,T;H)\to \mathrm{L}^\infty(0,T;H)$ is well defined, uniformly bounded, order preserving and Lipschitz continuous in the following sense: there exits $C>0$ such that:

$$\|\mathcal{F}(u,\xi)-\mathcal{F}(v,\xi)\|_{\mathrm{L}^\infty(0,T;H)}\leq C\,\|u-v\|_{\mathrm{L}^2(0,T;H)}\,.$$

The next result shows the existence of solution to problem (27). The proof is carried out through three different steps: time discretization, a priori estimates and passage to the limit by using compactness (cf. H.3). This approximation procedure is often used in the analysis of equations that include a memory operator since at any time-step we solve a stationary problem in which this operator is reduced to a standard nonlinear mapping (see, for instance, [46]).

Theorem 4.1. *Let us assume H.1, H.2 and H.3 hold true. Then, problem* (27) *has a solution.*

Proof. Let us fix $m\in\mathbb{N}$ and set $\Delta t:=T/m$. For $n=1,\dots,m$, we define $t^n:=n\Delta t$. The time discretization of problem (27) based on backward Euler's scheme reads as follows: given $u^0=u_0$ and $w^0=w_0$ in Ω, find $u^n\in V$ and $w^n\in H$, $n=1,\dots,m$, satisfying

$$(u^n+w^n,v)_{H,H}+\Delta t a(t^n,u^n,v)=\Delta t\langle f^n,v\rangle_{V,V'}+(u^{n-1}+w^{n-1},v), \tag{29}$$

$$w^n=[\mathcal{F}(u_{\Delta t^n},\xi)](t^n) \qquad \text{in } \Omega, \tag{30}$$

for all $v\in V$, where $u_{\Delta t^n}$ is the piecewise linear in time interpolant of $\{u^i\}_{i=0}^n$. In order to study the time-discrete problem we introduce the operator $F^n: H\longrightarrow H$ by

$$F^n(w):=[\mathcal{F}(\Lambda^n(w),\xi)](t^n) \quad \forall w\in H,$$

where $\Lambda^n: H\to \mathrm{H}^1(0,t^n;H)$ is defined as follows: for $w\in H$, $\Lambda^n(w)$ is the continuous piecewise linear function in time such that $\Lambda^n(w)(t^i)=u^i$, $i=0,\dots,n-1$, and $\Lambda^n(w)(t^n)=w$. From H.3 it follows that F^n is Lipschitz continuous in H, uniformly bounded and, from the order preservation property,

$$\left(F^n(w_1)-F^n(w_2)\right)(w_1-w_2)\geq 0 \quad \text{a.e. in } \Omega, \quad \forall w_1,w_2\in H. \tag{31}$$

Thus, from H.1 it follows that (29) has a unique solution (see, for instance, [42]). The next step is to prove an a priori estimate for the solution of (29). Let us apply (29) to $v = u^n - u^{n-1}$. For $n = 1, \dots, m$ we obtain

$$\Delta t \left\| \frac{u^n - u^{n-1}}{\Delta t} \right\|_H^2 + \left(\frac{w^n - w^{n-1}}{\Delta t}, u^n - u^{n-1} \right)_{H,H} + a(t^n, u^n, u^n - u^{n-1}) = \langle f^n, u^n - u^{n-1} \rangle_{V,V'}. \tag{32}$$

It is well known that, when the classical Preisach model is considered, the second term on the left hand side of the previous equality is positive. This is a consequence of the order preservation property and the fact that $w^{n-1} = F^n(u^{n-1})$ in the rate-independent setting. However, this does not hold true for the dynamic Preisach operator. In order to estimate this term, we first notice from (31) that, a.e. in Ω,

$$\begin{aligned}(w^n - w^{n-1})(u^n - u^{n-1}) &= (F^n(u^n) - F^n(u^{n-1}))(u^n - u^{n-1}) \\ &\quad - (w^{n-1} - F^n(u^{n-1}))(u^n - u^{n-1}) \\ &\geq -([\mathcal{F}(u_{\Delta t^n}, \xi)](t^{n-1}) - F^n(u^{n-1}))(u^n - u^{n-1}) \\ &= ([\mathcal{F}(\widetilde{u}_{\Delta t^n}, \xi)](t^n) - [\mathcal{F}(\widetilde{u}_{\Delta t^n}, \xi)](t^{n-1}))(u^n - u^{n-1}),\end{aligned} \tag{33}$$

where $\widetilde{u}_{\Delta t^n}$ is the continuous piecewise linear in time function such that $\widetilde{u}_{\Delta t^n}(t^i) = u^i$, $i = 0, \dots, n-1$ and $\widetilde{u}_{\Delta t^n}(t^n) = u^{n-1}$ a.e. in Ω. Moreover, from (22) and (26) it follows that, a.e. in Ω,

$$\begin{aligned}[\mathcal{F}(\widetilde{u}_{\Delta t^n}, \xi)](t^n) - [\mathcal{F}(\widetilde{u}_{\Delta t^n}, \xi)](t^{n-1}) &= \int_{t^{n-1}}^{t^n} \partial_t [\mathcal{F}(\widetilde{u}_{\Delta t^n}, \xi)](s) ds \\ = \int_{t^{n-1}}^{t^n} \int_{\mathcal{T}} \partial_t \eta_\rho(\widetilde{u}_{\Delta t^n}, \xi)(s) p(\rho) d\rho \, ds &\leq C \Delta t \left(|u^{n-1}| + 1 \right)\end{aligned} \tag{34}$$

where the last inequality follows from (4) and the fact that $\widetilde{u}_{\Delta t^n} = u^{n-1}$ in $[t^{n-1}, t^n]$. Here C depends on k but it is independent of Δt. On the other hand, in order to estimate the last term on the left-hand side of (32) we use the identity $2(p - q)p = p^2 + (p - q)^2 - q^2$ and the Lipschitz continuity of $a(\cdot, v, w) : (0, T) \to \mathbb{R}, \forall v, w \in V$ to obtain that

$$\begin{aligned}2a(t^n, u^n, u^n - u^{n-1}) &\geq a(t^n, u^n, u^n) - a(t^n, u^{n-1}, u^{n-1}) \\ &\geq a(t^n, u^n, u^n) - a(t^{n-1}, u^{n-1}, u^{n-1}) - C \Delta t \left\| u^{n-1} \right\|_V^2.\end{aligned} \tag{35}$$

Summing up (32) for $n = 1, \dots, l$ with $l \in \{1, \dots, m\}$ and by using (33)–(35) we obtain

$$\sum_{n=1}^{l} \Delta t \left\| \frac{u^n - u^{n-1}}{\Delta t} \right\|_H^2 + \frac{1}{2} a(t^l, u^l, u^l) \leq \frac{1}{2} a(t^0, u_0, u_0) + \sum_{n=1}^{l} C \Delta t \left\| u^{n-1} \right\|_V^2 + \sum_{n=1}^{l} \langle f^n, u^n - u^{n-1} \rangle_{V,V'} + C.$$

By proceeding as in [4] it follows that, for $l = 1, \dots, m$

$$\Delta t \sum_{n=1}^{l} \left\| \frac{w^n - w^{n-1}}{\Delta t} \right\|_H^2 + \Delta t \sum_{n=1}^{l} \left\| \frac{u^n - u^{n-1}}{\Delta t} \right\|_H^2 + \left\| u^l \right\|_V^2 \leq C. \tag{36}$$

Finally, let us define $u_{\Delta t} : [0,T] \to V$, $w_{\Delta t} : [0,T] \to H$ as the continuous piecewise linear in time interpolants of $\{w^n\}_{n=0}^m$ and $\{u^n\}_{n=0}^m$, respectively. We also introduce the step function $\overline{u}_{\Delta t} : [0,T] \to V$ by

$$\overline{u}_{\Delta t}(t^0) := u_0; \quad \overline{u}_{\Delta t}(t) := u^n, \quad t \in (t^{n-1}, t^n], \quad i = n, \dots, m,$$

and define the step functions $\overline{a}(t)$ and $\overline{f}$ in a similar way.

Using the above notation we rewrite equation (29) as follows:

$$(\partial_t u_{\Delta t} + \partial_t w_{\Delta t}, v)_{H,H} + \overline{a}(t, \overline{u}_{\Delta t}, v) = \langle \overline{f}, v \rangle_{V,V'} \quad \forall v \in V, \text{ a.e. in } (0,T]. \tag{37}$$

From (36) we deduce that there exists $C > 0$ such that

$$\|w_{\Delta t}\|_{\mathrm{L}^\infty(0,T;H)} + \left\| \frac{\partial w_{\Delta t}}{\partial t} \right\|_{\mathrm{L}^2(0,T;V')} + \|u_{\Delta t}\|_{\mathrm{H}^1(0,T;H)\cap \mathrm{L}^\infty(0,T;V)} + \|\overline{u}_{\Delta t}\|_{\mathrm{L}^\infty(0,T;V)} \leq C.$$

Thus, there exists u, w such that $w_{\Delta t} \to w$ and $u_{\Delta t} \to u$ weakly in the corresponding spaces. Passing to the limit in (37) we obtain

$$\langle \partial_t u + \partial_t w, v \rangle_{V,V'} + a(t, u, v) = \langle f, v \rangle_{V,V'} \qquad \forall v \in V, \quad \text{a.e. in } (0,T].$$

The next step is to prove that $w = \mathcal{F}(u, \xi)$. This equality follows from the compact embedding of $\mathrm{H}^1(0,T;H) \cap \mathrm{L}^2(0,T;V)$ in $\mathrm{L}^2(0,T;H)$ (see, for instance, [30, Th. 51]) and the Lipschitz continuity of $\mathcal{F}$ (see H.3). □

Remark 3. We are not aware of an uniqueness result for an abstract problem such as problem (27). However, uniqueness of solution has been shown for second order parabolic problems with hysteresis based on the generalized play operator (see, for instance, Visintin [46, Cor. IX.2.9]). The proof relies upon the Hilpert's inequality [21] for the *play* operator. Since the dynamic Preisach operator (22) satisfies the Hilpert's inequality (see (24)), following the same techniques as in [21, Theorem 5], it can be proved that there exists a unique solution to problem (27) when $a(t, u, v) = A(t, x)\nabla u \cdot \nabla v + \mathbf{b}(t, x) \cdot \nabla u v + c(t, x) u v$, with regular coeficients such that (28) holds true.

Example 4.2. *The previous result applies, for instance, to the parabolic equations below which arise in electromagnetism. More precisely, they are models to compute eddy currents in two-dimensional or axisymmetric domains filled with conducting ferromagnetic materials with hysteresis.*

$$\begin{aligned} \langle \partial_t u + \partial_t w, v \rangle_{V,V'} + (\nabla u, \nabla v)_{H,H} &= \langle f, v \rangle_{V,V'} \quad \forall v \in V, \quad \textit{a.e. in } (0,T], \\ w &= \mathcal{F}(u, \xi) \qquad \textit{in } \Omega \times [0,T], \\ (u + w)(0) &= u_0 + w_0 \qquad \textit{in } \Omega, \end{aligned}$$

where $V = \mathrm{H}^1_0(\Omega)$ and $H = \mathrm{L}^2(\Omega)$ (see Chapter IX in [46] for the rate-independent case).

It can also be applied to the axisymmetric eddy current model

$$\langle \partial_t w, rv\rangle_{V,V'} + \int_\Omega \frac{1}{\sigma r}\left(\frac{\partial(ru)}{\partial r}\frac{\partial(rv)}{\partial r} + \frac{\partial(ru)}{\partial z}\frac{\partial(rv)}{\partial r}\right) drdz = b'(t)\,(rv)\,|_\Gamma \quad \forall v \in V,$$
$$w = u + \mathcal{F}(u,\xi) \quad \text{in } \Omega \times (0,T),$$
$$w(0) = w_0 \quad \text{in } \Omega,$$

where $V = \left\{v \in \mathrm{L}^2_r(\Omega) : \partial_r(rv) \in \mathrm{L}^2_{1/r}(\Omega), \partial_z v \in \mathrm{L}^2_r(\Omega) \text{ and } rv|_\Gamma \text{ is constant}\right\}$ and $H = \mathrm{L}^2_r(\Omega)$. Here u represents the magnetic field, w is the magnetic induction, b is the magnetic flux and σ is the electrical conductivity (see [45]).

5. Numerical approximation and examples

The aim of this section is twofold: first, to introduce and analyze the convergence properties of a numerical scheme to approximate a partial differential equation (PDE) with hysteresis. For this purpose, we apply the numerical approximation to a test problem where several successively refined meshes and time-steps have been considered. Second, to illustrate the behavior of the numerical solution for different configurations of the dynamic Preisach model.

With this end, let us consider the following weak formulation: find $u \in \mathrm{H}^1(0,T;\mathrm{L}^2(\Omega)) \cap \mathrm{L}^\infty(0,T;\mathrm{H}^1(\Omega))$ and $w \in \mathrm{L}^2(0,T;\mathrm{L}^2(\Omega))$ with $\partial_t w \in \mathrm{L}^2(0,T;\mathrm{H}^1(\Omega)')$, such that

$$\langle \partial_t u + \partial_t w, v\rangle_{\mathrm{H}^1(\Omega),\mathrm{H}^1(\Omega)'} + \sigma^{-1}(\nabla u, \nabla v) = 0 \qquad \forall v \in \mathrm{H}^1_0(\Omega), \tag{38a}$$
$$w = \mathcal{F}(u,\xi) \qquad \text{in } \Omega \times [0,T], \tag{38b}$$
$$u = g \qquad \text{on } \partial\Omega \times [0,T], \tag{38c}$$
$$(u+w)(0) = 0 \qquad \text{in } \Omega, \tag{38d}$$

where $\Omega \in \mathbb{R}^2$, $\sigma > 0$ and $g \in \mathrm{H}^1(0,T;\mathrm{H}^{1/2}(\Gamma))$. This problem arises, for instance, in the computation of 2D electromagnetic field in a cross-section of laminated media (see [45]). This field is important for the evaluation of the electromagnetic losses.

Notice that this problem does not lie exactly in the previous framework because Dirichlet, instead of Neumann, boundary condition are prescribed. Nevertheless, the existence of solution can be proved with the same techniques as those in [4].

Next, we introduce a fully discrete approximation of problem (38). From now on we will assume that Ω is a convex polygon. We associate a family of partitions $\{\mathcal{T}_h\}_{h>0}$ of Ω into triangles, where h denotes the mesh size. Let $\mathcal{V}_h$ be the space of continuous piecewise linear finite elements. We also consider the finite-dimensional space $\mathcal{V}^0_h := \mathcal{V}_h \cap \mathrm{H}^1_0(\Omega)$ and denote by $\mathcal{V}_h(\Gamma)$ the space of traces on Γ of functions in $\mathcal{V}_h$. We introduce a uniform partition $\{t^i := i\Delta t, i = 0,\ldots,m\}$ of $[0,T]$, with time step $t := T/m, m \in \mathbb{N}$. By using the above finite element space for space discretization and the backward Euler scheme for time discretization, we are led to the following Galerkin approximation of problem (38): Given $u_h^0 = w_h^0 = 0$ in Ω, find $u_h^n \in \mathcal{V}_h$ and $w_h^n \in \mathcal{V}_h$, $n = 1, \ldots, m$, satisfying

$$(u_h^n + w_h^n, v_h) + \Delta t \sigma^{-1}(\nabla u_h^n, \nabla v_h) = (u_h^{n-1} + w_h^{n-1}, v_h) \quad \forall v_h \in \mathcal{V}_h^0, \tag{39a}$$

$$w_h^n = [\mathcal{F}(u_{\Delta t^n}^h, \xi)](t^n) \quad \text{in } \Omega, \tag{39b}$$

$$u_h^n = g_h^n \quad \text{in } \Gamma, \tag{39c}$$

where $g_h^n \in \mathcal{V}_h(\Gamma)$ is a convenient approximation of $g(t^n), n = 1, \ldots, m$ and $u_{\Delta t^n}^h$ is the piecewise linear in time interpolant of $\{u_h^i\}_{i=0}^n$.

At each time step of the above algorithm, we must solve a non-linear problem. With this purpose, and given the history dependence of the nonlinear operator, we have considered a Newton-like method. To complete the proposed numerical scheme, a particular hysteresis operator must be considered (cf. (39b)). In view of applications we have considered the dynamic Preisach model described in Section 3 characterized by the Factorized-Lorentzian distribution (25) (see Figure 5 (right)) and different values of slopes k (cf. (4)).

5.1. Convergence analysis

Given the difficulties related with the numerical analysis of the problem, we estimate experimentally the order of convergence of the scheme presented in the previous section. With this aim, we have solved problem (39) in a square domain $\Omega = [0, 0.02]^2$ along the time interval $[0, 0.01]$, with $\sigma = 100$, non-homogeneous Dirichlet boundary condition $g(x, y, t) = 200 \sin(2\pi t/0.01)$ and the dynamic Preisach model with slope $k = 10$.

Since there is no analytical solution to this problem, we asses the performance of the method by comparing the computed results with those obtained with a very fine uniform mesh of size $h_0/15$ and time step $\Delta t_0/512$. The solution to this problem is taken as the "exact" solution u. The method has been used on several successively refined meshes chosen in a convenient way in order to analyze convergence. We denote by $h_0 = 0.0033$ the corresponding mesh size and we have taken as coarser time step $\Delta t_0 = 0.01$. The rest of the meshes are uniform refinements of this one. The numerical approximations are compared with the "exact" solution by computing the percentage error for u in both a discrete $\mathrm{L}^2(0, T; \mathrm{L}^2(\Omega))$-norm and a discrete $\mathrm{L}^2(0, T; \mathrm{H}^1(\Omega))$-semi norm, respectively.

Figure 8 (left) shows the percentage error for u versus the mesh-size h for a fixed time-step. We observe a linear order of convergence in norm $\mathrm{L}^2(0, T; \mathrm{H}^1(\Omega))$ and a quadratic order in $\mathrm{L}^2(0, T; \mathrm{L}^2(\Omega))$. A similar behavior is also observed when the rate-independent Preisach model is considered (see [3]).

5.2. Numerical solution for different k-values

In this section we illustrate the behavior of the numerical solution to problem (39) for different configurations of the dynamic Preisach model. As we notice in Section 3, the evolution of the dynamic relay and, accordingly, of the dynamic

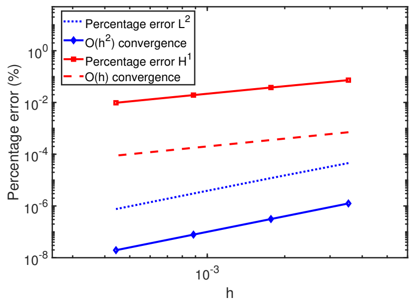

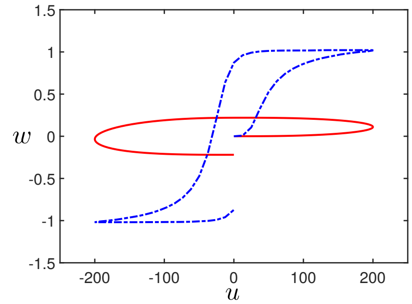

Figure 8: Left. Percentage errors in norms and versus the mesh-size h for a fixed time-step $\Delta t/128$ (log-log scale). Right. Curve $w-u$ on a boundary point for $k = 10^3$ (dashed line) and $k = 0$ (solid line).

Preisach model, varies with respect to the velocity of the input and the relay slope k (cf. Figures 2, 3 and 7). We have computed the solution to problem (39) for two different values of the slope k of the dynamic Preisach model; in particular, those corresponding to $k = 1$ and $k = 10^3$. Figures 9 and 10 show fields u and w solution to problem (39). From Figure 10 (bottom) it can be seen that changes in w are smaller when $k = 1$. This behavior is expected as the size of the $u - w$ cycle decreases when the slope k decreases (see Figure 2). This is not the case for the w field if $k = 10^3$: it reaches values close to saturation (see Figures 10 (top) and 8 (right)).

Remark 4. Let us make some consideration regarding electromagnetic losses. Traditionally, the total losses are divided into classical eddy current losses and hysteresis losses. The former can be computed with the well-known formula

$$\int_\Omega \mathbf{J}(x,t) \cdot \mathbf{E}(x,t)\, dx \quad \text{(W)}$$

while the latter are related to the area enclosed by the loops in the (H,B) "plane". Both can be computed by finite element solution of eddy current models combined, for instance, with the *classical* Preisach model for hysteresis but there also exist much simpler approximate formulas involving coefficients that needs to be identified for each particular material (see, for instance, [49]). However, for high to moderate frequencies, the sum of classical eddy current losses and the (rate-independent) hysteresis losses has revealed to underestimate the total experimental losses. This fact has lead to conjecture the existence of additional losses that are called *excess eddy current losses* as they are supposed to be a consequence of rate-dependent phenomena other than the Joule (or classical eddy current) losses. Therefore, the use of rate-dependent hysteresis models as the dynamic Preisach model by Bertotti [6] would seem to be more appropriated than the classical Preisach one.

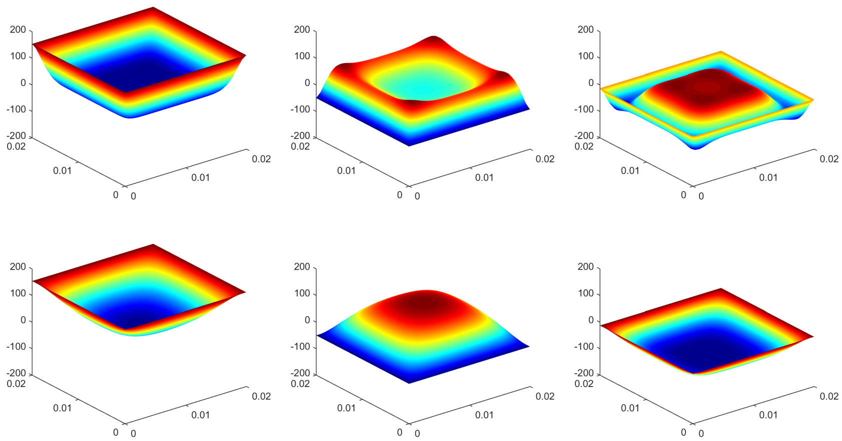

$t = 0.002$s $\qquad$ $t = 0.0055$s $\qquad$ $t = 0.01$s

Figure 9: u-field solution to problem (39) for $k = 10^3$ (top) and $k = 1$ (bottom).

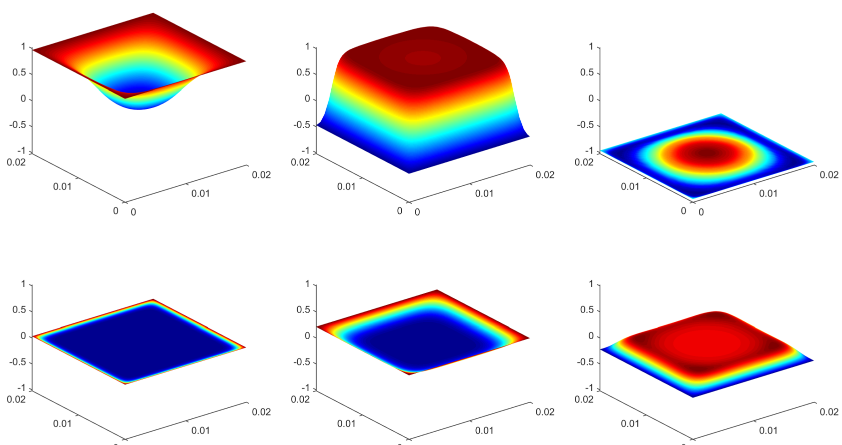

$t = 0.002$s $\qquad$ $t = 0.0055$s $\qquad$ $t = 0.01$s

Figure 10: w-field solution to problem (39) for $k = 10^3$ (top) and $k = 1$ (bottom).

6. Conclusion

In this paper, we have introduced a functional analytic framework to study the dynamic Preisach model presented in [6]. This framework allow us to prove properties of the operator that can be used to study a wide range of hysteresis phenomena. In particular, and motivated by electromagnetic field equations, we study the existence of a solution to a family of PDE's involving hysteresis. We have noticed that, even though the analysis is similar to the one applied for the classical Preisach model, key changes need to be done for the dynamic case. We also propose a numerical scheme to approximate a parabolic problem with dynamic hysteresis. The numerical results presented in sections 3 and 5 help us to become familiar with the role of the k-value and the speed of the input in the dynamic Preisach model and how this parameter affects the solution of a PDE. A better understanding of the dynamic behavior of solution in processes with hysteresis is essential to understand the process itself and to develop appropriate numerical approximations.

References

[1] F. Baronti, N. Femia, R. Saletti, C. Visone, and W. Zamboni. Hysteresis modeling in li-ion batteries. *IEEE Trans. Magn.*, 50(11):1–4, 2014.

[2] V. Basso, G. Bertotti, O. Bottauscio, F. Fiorillo, M. Pasquale, M. Chiampi, and M. Repetto. Power losses in magnetic laminations with hysteresis: Finite element modeling and experimental validation. *J. Appl. Phys.*, 81(8):5606–5608, 1997.

[3] A. Bermúdez, L. Dupré, D. Gómez, and P. Venegas. Electromagnetic computations with preisach hysteresis model. *Finite Elem. Anal. Des.*, 126:65–74, 2017.

[4] A. Bermúdez, D. Gómez, R. Rodríguez, and P. Venegas. Mathematical analysis and numerical solution of axisymmetric eddy-current problems with preisach hysteresis model. *Rend. Semin. Mat. Univ. Politec. Torino*, 72(1-2):73–117, 2014.

[5] A. Bermúdez and C. Moreno. Duality methods for solving variational inequalities. *Comput. Math. Appl.*, 7:43–58, 1981.

[6] G. Bertotti. Dynamic generalization of the scalar preisach model of hysteresis. *IEEE Trans. Magn.*, 28(5):2599–2601, 1992.

[7] G. Bertotti. *Hysteresis in Magnetism.* Academic Press, 1998.

[8] G. Bertotti and I. D. Mayergoyz, editors. *The Science of Hysteresis. Vol. I.* Elsevier/Academic Press, Amsterdam, 2006.

[9] G. Bertotti and M. Pasquale. Physical interpretation of induction and frequency dependence of power losses in soft magnetic materials. *IEEE Trans. Magn.*, 28(5):2787–2789, 1992.

[10] O. Bottauscio, M. Chiampi, D. Chiarabaglio, and M. Repetto. Preisach-type hysteresis models in magnetic field computation. *Physica B*, 275(1-3):34–39, 2000.

[11] H. Brézis. *Opérateurs maximaux monotones et semi-groupes de contractions dans les espaces de Hilbert*. North-Holland, 1973.

[12] M. Brokate and J. Sprekels. *Hysteresis and Phase Transitions*. Springer, Berlin, 1996.

[13] E. Della Torre. *Magnetic Hysteresis*. IEEE Press, New York, 1999.

[14] L. Dupré, G. Bertotti, V. Basso, F. Fiorillo, and J.A.A Melkebeek. Generalisation of the dynamic preisach model toward grain oriented FeSi alloys. *Physica B: Condensed Matter*, 275(1):202 – 206, 2000.

[15] L. Dupré, G. Bertotti, and J.A.A. Melkebeek. Dynamic preisach model and energy dissipation in soft magnetic materials. *IEEE Trans. Magn.*, 34(4, 1):1168–1170, 1998.

[16] M. Eleuteri. Well-posedness results for a class of partial differential equations with hysteresis arising in electromagnetism. *Nonlinear Anal-Real*, 8(5):1494 – 1511, 2007.

[17] M. Eleuteri and J. Kopfová. Uniqueness and decay estimates for a class of parabolic partial differential equations with hysteresis and convection. *Nonlinear Anal.*, 73(1):48–65, 2010.

[18] J. A. Ewing. X. experimental researches in magnetism. *Philos. Trans. R. Soc. Lond.*, 176:523–640, 1885.

[19] P. Gurevich and W. Jäger. Parabolic problems with the Preisach hysteresis operator in boundary conditions. *J. Differential Equations*, 247(11):2966–3010, 2009.

[20] V. Hassani, T. Tjahjowidodo, and N. D. Thanh. A survey on hysteresis modeling, identification and control. *Mech. Syst. Signal Proc.*, 49(1-2, SI):209–233, 2014.

[21] M. Hilpert. On uniqueness for evolution problems with hysteresis. In *Mathematical Models for Phase Change Problems*, volume 88 of *International Series of Numerical Mathematics*, pages 377–388. Birkhǎuser Basel, 1989.

[22] M. Hintermüller, K. Ito, and K. Kunisch. The primal-dual active set strategy as a semismooth Newton method. *SIAM J. Optim.*, 13(3):865–888 (2003), 2002.

[23] P. Kordulová. Water flow through unsaturated porous media with hysteresis. *Nonlinear Anal-Real*, 12(6):3125 – 3134, 2011.

[24] M.A. Krasnosel'skiĭ and A.V. Pokrovskiĭ. *Systems with Hysteresis*. Springer, Berlin, 1989. (Russian edition, Nauka, Moscow (1983)).

[25] P. Krejčí. *Hysteresis, convexity and dissipation in hyperbolic equations*, volume 8 of *GAKUTO Internat. Ser. Math. Sci. Appl.* Gakkōtosho Co., Ltd., Tokyo, 1996.

[26] P. Krejčí. Evolution variational inequalities and multidimensional hysteresis operators. In *Nonlinear differential equations*, volume 404 of *Res. Notes Math.*, pages 47–110. Chapman & Hall/CRC, London, 1999.

[27] P. Krejčí, J. P. O'Kane, A. Pokrovskii, and D. Rachinskii. Properties of solutions to a class of differential models incorporating Preisach hysteresis operator. *Phys. D*, 241(22):2010–2028, 2012.

[28] P. Krejčí, P. and V. Lovicar. Continuity of hysteresis operators in sobolev spaces. *Appl. Math.*, 35:60–66, 1990.

[29] M. Kuczmann. Dynamic Preisach model identification applying FEM and measured BH curve. *COMPEL*, 33(6):2043–2052, 2014.

[30] J.L. Lions. *Quelques méthodes de résolution des problèmes aux limites non linéaires*. Dunod, Gauthier-Villars, Paris, 1969.

[31] V. A. Lubarda, D. Šumarac, and D. Krajcinovic. Preisach model and hysteretic behaviour of ductile materials. *European J. Mech. A Solids*, 12(4):445–470, 1993.

[32] J. W. Macki, P. Nistri, and P. Zecca. Mathematical Models for Hysteresis. *SIAM Review*, 35(1):94–123, 1993.

[33] G. Marinoschi. The diffusive form of Richards' equation with hysteresis. *Nonlinear Anal-Real*, 9(2):518 – 535, 2008.

[34] I. D. Mayergoyz. Dynamic Preisach Model of hysteresis. *IEEE Trans. Magn.*, 24(6):2925–2927, 1988.

[35] I. D. Mayergoyz. *Mathematical models of hysteresis*. Springer-Verlag, New York, 1991.

[36] I. D. Mayergoyz. *Mathematical Models of Hysteresis and their applications*. Elsevier, 2003.

[37] A. Mielke and R. Rossi. Existence and uniqueness results for a class of rate-independent hysteresis problems. *Math. Models Meth. Appl. Sci.*, 17(01):81–123, 2007.

[38] J.J. Moreau. On unilateral constraints, friction and plasticity. In The editor, editor, *New variational techniques in mathematical physics (C.I.M.E. course, Bressanone, 1973*, volume 4 of *5*, chapter 8, pages 171–322. Edizione Cremonese, Roma, 3 edition, 7 1973. An optional note.

[39] D. A. Philips, L. Dupré, J. Cnops, and J. A. A. Melkebeek. The application of the preisach model in magnetodynamics: theoretical and practical aspects. *J. Magn. Magn. Mater.*, 133(1):540 – 543, 1994.

[40] F. Preisach. Über die magnetische nachwirkung. *Zeitschrift für Physik,*, 94:277–302, 1935.

[41] A. Rao and A.R. Srinivasa. A two species thermodynamic Preisach model for the torsional response of shape memory alloy wires and springs under superelastic conditions. *Int. J. Solids Struct.*, 50(6):887 – 898, 2013.

[42] T. Roubíček. *Non Linear Partial Differential Equations with Applications.* Birkhäuser, 2005.

[43] B. Schweizer. Hysteresis in porous media: Modelling and analysis. *Interface Free Bound.*, 19(3):417–447, 2017.

[44] R. E. Showalter, T. D. Little, and U. Hornung. Parabolic PDE with Hysteresis. *Control Cybern.*, 25:631–643, 1996.

[45] R. Van Keer, L. Dupré, and J. A. A. Melkebeek. On a numerical method for 2D magnetic field computations in a lamination with enforced total flux. *J. Comput. Appl. Math.*, 72:179–191, 1996.

[46] A. Visintin. *Differential models of hysteresis*, volume 111 of *Applied Mathematical Sciences*. Springer-Verlag, Berlin, 1994.

[47] A. Visintin. Chapter 1 - Mathematical Models of Hysteresis. In Giorgio Bertotti and I. D. Mayergoyz, editors, *The Science of Hysteresis*, pages 1 – 123. Academic Press, Oxford, 2006.

[48] Y. Yu, Z. Xiao, N. G. Naganathan, and R. V. Dukkipati. Dynamic preisach modelling of hysteresis for the piezoceramic actuator system. *Mech. Mach. Theory*, 37(1):75–89, 2002.

[49] Y. Zhang, M.-C. Cheng, and P. Pillay. In *2009 IEEE Industry Applications Society Annual Meeting.*